Characterization of the stretched-exponential trap-time distributions in one-dimensional coupled map lattices

S. I. Simdyankin,[1] Normand Mousseau,[1] and E. R. Hunt[2]

[1]*Département de Physique and Centre de Recherche en Physique et Technologie des Couches Minces, Université de Montréal, Case Postale 6128, Succursale Centre-ville, Montréal, Québec, Canada H3C 3J7*

[2]*Department of Physics and Astronomy and CMSS, Ohio University, Athens, Ohio 45701*

(Received 20 August 2002; published 12 December 2002)

Stretched-exponential distributions and relaxation responses are encountered in a wide range of physical systems such as glasses, polymers, and spin glasses. As found recently, this type of behavior occurs also for the distribution function of a certain trap time in a number of coupled dynamical systems. We analyze a one-dimensional mathematical model of coupled chaotic oscillators that reproduces an experimental setup of coupled diode resonators and identify the necessary ingredients for stretched-exponential distributions.

I. INTRODUCTION

The decay of certain quantities characteristic of many complex systems, such as glasses [1], spin glasses [2], quasicrystals [3], trapping models [4–6], coupled nonlinear systems [7–9], turbulence [10,11], and others [12–14] is often described by a stretched-exponential (or Kohlrausch) functional form:

$$\phi(t) = \exp[-(t/\tau)^\beta], \quad t \geq 0, \tag{1}$$

with $0 < \beta < 1$ [15]. Although Eq. (1) provides a good fit to a wide range of experimental and numerical results, in many cases, these can also be fitted by power laws with comparable accuracy; while most experimental setups can span many decades in time, few have achieved more than 2 or 3 decades in $\phi(t)$. The Kohlrausch form can also be reproduced explicitly by a few theoretical models (see, e.g., Refs. [2,4,5,16,17]) on the basis of various assumptions, but it is still unclear whether there can be a unifying solid theoretical justification for it.

Recently, Hunt, Gade, and Mousseau [7] found that stretched exponentials could fit experimental distributions of trap time—the time a system spends in an uninterrupted state with temporal period two, in a one-dimensional network of coupled diode resonators—over more than 6 decades in the distribution. Numerical models, based on this setup, could expand this fitting over about ten orders of magnitude, strongly suggesting that dynamics with underlying stretched-exponential distributions could be universal in coupled chaotic systems and ruling out a power-law or any other standard fit.

In this paper, we revisit one such numerical model and provide a detailed characterization of the dynamics of this network as a function of system size and parameters, providing elements of explanation regarding the origin of stretched-exponential distributions in this system. In particular, we show that (1) size effects are important only for relatively small systems; (2) the natural invariant density, $\rho(x)$, generated by typical orbits has well-defined structure that is self organized; (3) the structure of $\rho(x)$ alone cannot lead to stretched-exponential distributions—the dynamical spatial organization is essential for stabilizing the periodic orbits.

This paper is organized as follows. In the following section, we introduce the mathematical model: a one-dimensional coupled map lattice. Section III discusses the background for the trap-time distributions. In Sec. IV, the results from the simulation are presented, to be discussed in Sec. V. We summarize our conclusions in Sec. VI.

II. MODEL

Our model is a one-dimensional chain of N diffusively coupled nonlinear deterministic maps, $f(x)$, with a coupling constant α and periodic boundary conditions. The interaction is totalistic and involves only the nearest neighbors. The time evolution of this system is discrete and is described by an iterative equation:

$$x_n(t+1) = (1-\alpha)f(x_n(t)) + \frac{\alpha}{2}\{f(x_{n-1}(t)) + f(x_{n+1}(t))\}, \tag{2}$$

which, given initial conditions $x_n(0)$ for each site $n = 1,2,\ldots,N$, generates a time series $\{x_n(t)\}$, for integer values of the time index $t = 0,1,\ldots$. This model offers a much simplified version of the one-dimensional array of diode resonators studied in Refs. [18–21]. Although the individual diode resonators are best described by an inertial equation [22], it was shown recently that Eq. (2) captures the dynamics in the regime of interest here [7].

The diffusive nature of the coupling in Eq. (2) becomes more apparent if this equation is rewritten in the following form:

$$x_n(t+1) = f(x_n(t)) + \frac{\alpha}{2}\{f(x_{n-1}(t)) - 2f(x_n(t))$$

$$+ f(x_{n+1}(t))\}$$

$$= f(x_n(t)) + \frac{\alpha}{2}D_+D_-f(x_n(t)), \tag{3}$$

where the central difference operator $D_+ D_- f(x_n)$ is the discrete Laplacian of $f(x_n)$ on a one-dimensional grid with unit spacing. In the limit $N \rightarrow \infty$, the discrete Laplacian can be substituted by its continuous counterpart and Eq. (3) becomes a nonlinear analog of a difference-differential diffusion equation, see, e.g., Ref. [23].

We use the logistic map $f(x) = rx(1-x)$, Ref. [24], in order to describe the dynamics of the basic chaotic elements. Although this differs from the form studied in Ref. [7], $g(y) = 1 - ay^2$, the results are unaffected; the two maps are conjugate, related by a simple algebraic transformation: $x = \sqrt{a}y/\sqrt{r} + 1/2$, $g(y) = f(x(y)) - r/4 + 1$. We choose the logistic map because it is more studied in the literature. In the simulations presented here, we fix the value of the coupling constant to $\alpha = 0.25$, and vary N and r, which we refer to as the nonlinearity parameter in the following. For a large N, $1/r$ can be thought of as a "viscosity" and α as a "diffusivity" with their usual relation to the "temperature."

Initial values of $x_n(0)$ are taken from a random distribution in the $[0,1[$ interval. Runs are then iterated for a few hundred thousand steps in order to avoid any transient effect before starting the accumulation of data. All the simulations presented here are done on one-dimensional arrays with variable length and periodic-boundary conditions. Statistics are generally accumulated over 10^7–10^{10} time steps.

Following the experiment [7], the analysis of the dynamics is done using coarse-grained variables defined by

$$\sigma_n(t) = \text{sgn}[x_n(t) - x_{\text{thr}}], \quad t = 0, 2, 4, \ldots, \tag{4}$$

where the quantity $x_n(t)$ is defined in Eq. (2) and x_{thr} is a certain threshold value. The results presented here are not very sensitive to the value of the threshold. For simplicity, we select the value of the unstable fixed point, $x_* = 1 - 1/r$, for the single map. This coarse graining reduces the problem from continuous to two state.

The basic dynamics of the coupled oscillator being period 2, the analysis is also done only over even (or odd) time steps.

III. BACKGROUND: THE DISTRIBUTION OF TRAP TIME

We are interested in the statistical distribution $\rho(t)$ of trap time in a coarse-grained state space of a one-dimensional chain of coupled nonlinear maps, as shown in Fig. 1. This quantity is formally equivalent to the distribution of time intervals between zero crossings of renewal processes, such as random walks [25] and has the advantage that it can be measured experimentally and numerically to a high degree of accuracy for this system [7].

Generally, however, experimentally measurable relaxation responses are mathematically described by autocorrelation functions of certain dynamical variables. For example, the inverse Fourier transform of the dynamical structure factor, the intermediate scattering function, can be calculated as the time autocorrelation function of the microscopic density distribution of particles in a material [26].

The relation between the autocorrelation function $C(t) = \langle \sigma(t') \sigma(t'+t) \rangle_{t'}$ of a renewal process $\sigma(t)$—defined
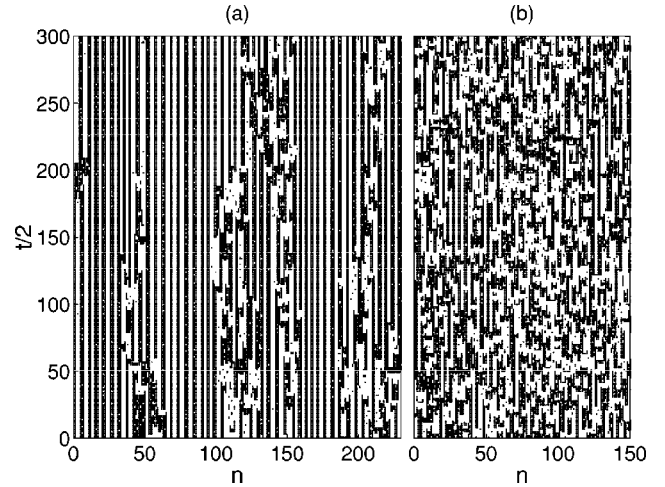

FIG. 1. Coarse-grained time evolution of the coupled logistic map. The coarse-grained variable $\sigma_n(t)$ in a stroboscopic representation: for every other iteration t, a dot at (n,t) corresponds to $\sigma_n(t) = +1$ and the blank space signifies $\sigma_n(t) = -1$. $N = 1000$ and (a) $r = 3.83$, (b) $r = 3.8888$.

analogously to Eq. (4)—and the distribution of trap time of this process was recently studied for a range of distributions [25]. Using this framework, it is possible to show that $C(t)$ corresponding to the stretched-exponential distribution of the occupation time is also a stretched exponential at long time, albeit with a different stretching exponent β.

These results are only valid when the traps are uncorrelated in time, which is the case for the systems studied here. The details of this work will be presented elsewhere [27].

This establishes a direct relation between the distribution of trap time, discussed in this paper, and the more standard autocorrelation function, measured in a number of experiments on glasses and other complex systems.

IV. RESULTS

Before discussing the possible origins for the stretched-exponential distributions in our model, it is necessary to offer a characterization of its dynamics as a function of the parameters of the model.

First, we consider the size effects on the dynamics of the network, studying experimental setup, varying in length between 15 and 256 oscillators, and simulated arrays of up to tens of thousands of sites.

Then we investigate the dynamics of the system as a function of the nonlinearity parameter r, which brings the system through a series of dynamical changes from stable periodic orbits to full chaos. In particular, it is important to assess the parts of the parameter space, where the stretched-exponential distributions can be observed.

Once the basic phase diagram is established, we discuss the building up of the dynamics on a single site embedded in the network as well as the spatial structure associated with the stretched-exponential distribution.

A. Dependence on N

As is seen in Fig. 1, the traps are directly associated with a periodic spatial organization, which is controlled by the coupling α.
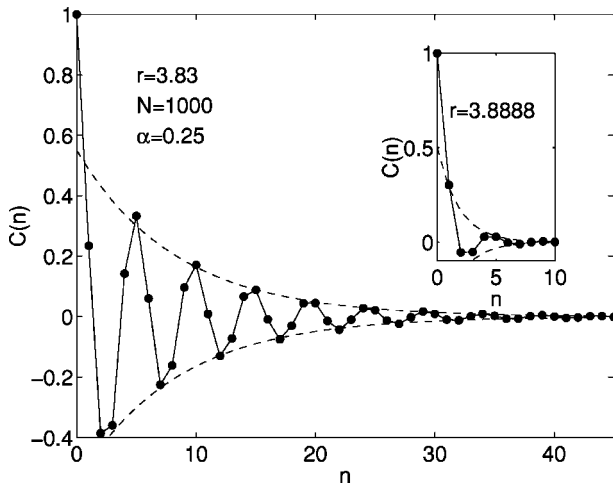
FIG. 2. Spatial correlation function $C(n)$ $= \langle \sigma_{n'}(t) \sigma_{n+n'}(t) \rangle_{n',t}$. Dots correspond to the numerical data. The solid line interpolates numerical points and is shown as a guide to the eye. The dashed lines show the exponential decay of oscillations: $\pm 0.55 \exp(-n/8.25)$. The inset also shows $C(n)$, but calculated for a different value of r. The amplitude of oscillations (dashed lines) in this case decays as $\pm 0.5 \exp(-n/1.8)$.

As α is increased, the spatial organization goes through two rapid transitions, showing qualitatively different features: For $\alpha < 0.1$, the lattice tends to follow a period-2 spatial organization. For intermediate values of $0.1 < \alpha < 0.19$, the lattice immediately freezes into a period-2 state in both space and time, for all values of the driving parameter, r. Above this threshold, $\alpha > 0.19$, the dynamics becomes stochastic again, while dominant spatial period goes to 4 and even longer for large α. In each of these phases, the variation of α affects only minimally the spatial structure of the phase.

In spite of the evident organization seen in Fig. 1, the spatial correlation is short range. Figure 2 shows that spatial correlations vanish exponentially fast with a typical length scale between about 2 and 8, i.e., the only static spatial correlation appearing in the system is directly associated with the short-range organization.

This short-range correlation implies that size effects should be very limited. Figure 3 shows the lattice-size dependence on the bifurcation diagram, for a single site on the lattice.

For small lattices, $1 < N < 32$, the dynamics depends on whether N is even or odd. For even N, arrays synchronize rapidly while the odd sizes continue to display chaotic trajectories. For example, the bifurcation diagram changes qualitatively as one goes from a single isolated site to a chain of 8 or 16 oscillators: the chaotic phase disappears totally and the system remains periodic in the coarse-grained state space until $r = 4.0$ [see Fig. 3(b)]. While isolated oscillators produce an exponential trap-time distribution, this distribution tends to the stretched-exponential form at short times for lattices with odd N as small as 15. Size effects are still present for these lattices, however, and the long-time distribution diverges from the stretched exponential [see Fig. 4(a)]. Interestingly, the sign of the deviation for the stretched exponential oscillates, as the array is increased in size 2×2, indicating a certain spatial frustration in these small systems.

For even N that is not a multiple of four, the mismatch with the periodicity results in the presence of inclusions of stable defects, with four sites in a row in the same band. These defects can also be present and be stable in lattices, where N is a multiple of four.

As the number of elements reaches 32, orbits corresponding to larger values of $r_{min} \leq r \leq 4$ become chaotic and the bifurcation diagram approaches that of an infinite lattice. r_{min} continues to decrease with growing number of sites, and is well converged for a lattice of a few hundred oscillators. As shown in Fig. 4(b) the same trend is seen experimentally,
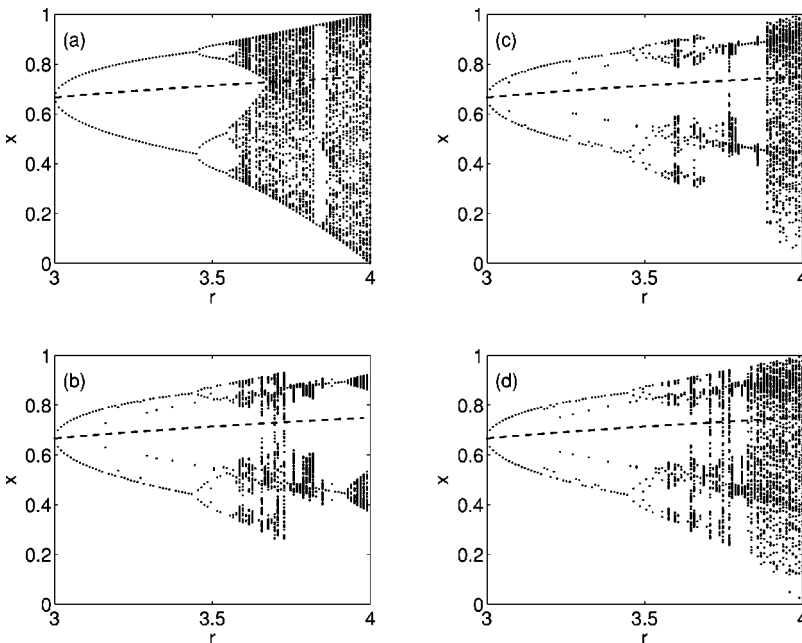

FIG. 3. Bifurcation diagrams for (a) an isolated map, (b) $N = 16$, (c) $N = 32$, and (d) $N = 10\,000$. The dashed line in all panels shows the unstable orbit $x_* = 1 - 1/r$.
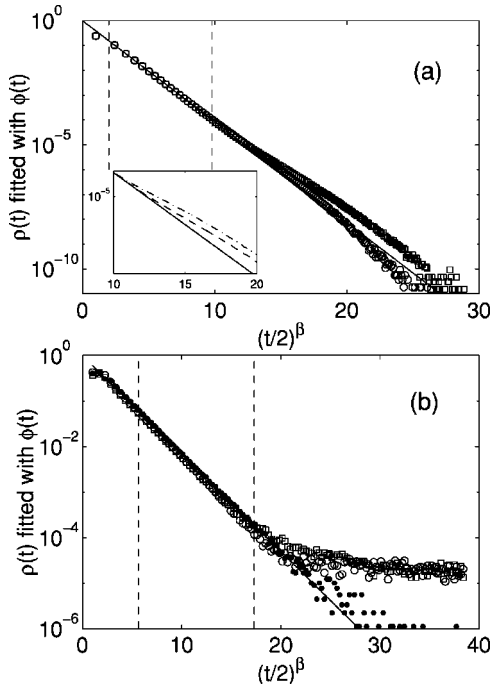
FIG. 4. (a) Distribution of trap time for $r=3.8888$. $N=21$ (squares: set of data points lying above the solid line) and $N=19$ (open circles: the set of data points lying below the solid line). The solid line corresponds to the stretched-exponential fit Eq. (1) with $\beta=0.50\pm0.05$ and $\tau=3.0\pm0.5$. In the inset, we show the data for $N=17$ (dash-dotted line), $N=21$ (dashed line), and the fit (solid line). (b) Distribution of trap time for the experimental setup (squares, $N=21$; dots, $N=20$; open circles, $N=19$). The stretched-exponential fit is with $\beta=0.75\pm0.05$ and $\tau=5.0\pm0.5$. Vertical lines in both panels demarcate the interval, over which the fitting procedure was performed.

although the inherent disorders help to decrease the finite size effects.

Even though the bifurcation diagrams for an isolated map and the infinite lattice appear similar, their respective orbits are qualitatively different for most values of r. In particular, most of the chaotic region of the latter shows a stretched-exponential trap-time distribution.

B. Dependence on r

Figure 3 also indicates the effect of r on the dynamics of a single site in a chain. The coupling stabilizes the orbits, reducing significantly the size of the chaotic region. Its effect is to shift the bifurcation diagram to the right, moving the dynamics towards periodic orbits as is shown in Fig. 5 (Fig. 5 will be discussed in more detail in Sec. IV C).

The stretched-exponential behavior appears, for a large enough lattice, around $r_0=3.83$. At this threshold value, the stretching exponent $\beta\approx0.33$, obtained from fitting the long-time part of the trap distribution (Fig. 6), according to Eq. (1). 0.33 is the lowest value of β, we could observe for the explored regions of the parameter space of the model. Below this threshold, chaotic windows are interspersed with periodic ones. Trajectories in these narrow windows tend to fall erratically into neighboring periodic orbits, generating
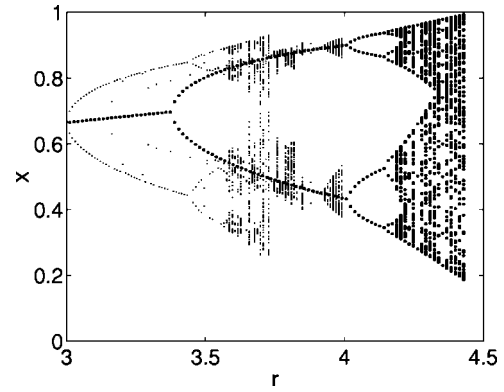

FIG. 5. Larger dots: bifurcation diagram of the map $x(t+1)=0.75f(x(t))+0.1625$. Smaller dots: the same as in Fig. 3(b). Although $\rho(a)$ [dashed-dotted line in Fig. 7(c)] corresponding to the bifurcation diagram depicted by the smaller dots is not a δ function, it is narrow enough so that it creates a period-2 attractor in the coarse grained phase space of the couple map chain.

multiple-step trap distributions with no clear overall time behavior.

As seen in Fig. 6, the value of β increases with r. For $r=3.8888$, the trap-time distribution is well fitted by a stretched exponential with $\beta\approx0.5$, while at $r=4$, the full chaos limit for an isolated logistic map, a fit to $\rho(t)$ gives $\beta=0.70\pm0.05$ and $\tau=3.0\pm0.5$.

Because of the short spatial correlation and the excellent quality of the simulation data, the exact value of β is well defined: increasing the lattice size from 64 to 1000 sites leaves the trap distribution essentially unchanged. Moreover, the same values of β are obtained, within the error bars, by changing the length of the interval, over which the fitting procedure is performed.

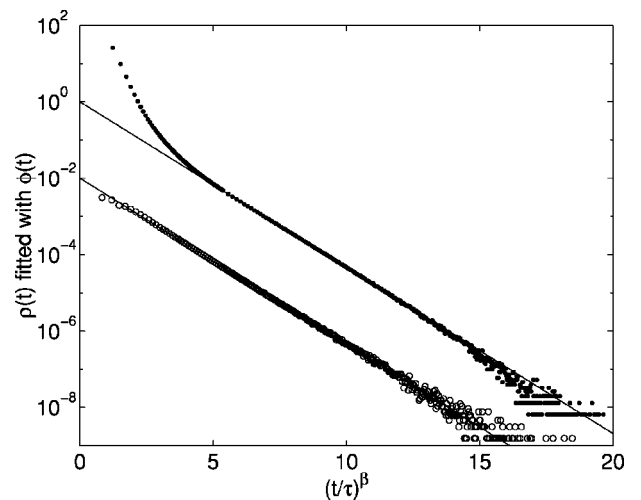These numbers are also in reasonable agreement with experimental results, which show β varying from (0.10

FIG. 6. Trap-time distributions fitted with stretched exponentials. Dots correspond to $N=1000$, $r=3.83$ and $\beta=0.33\pm0.05$, $\tau=11.5\pm0.5$. Open circles correspond to $N=64$, $r=3.8888$, and $\beta=0.50\pm0.05$, $\tau=2.9\pm0.5$. The solid lines show the best fit to the stretched-exponential function $\phi(t)$.
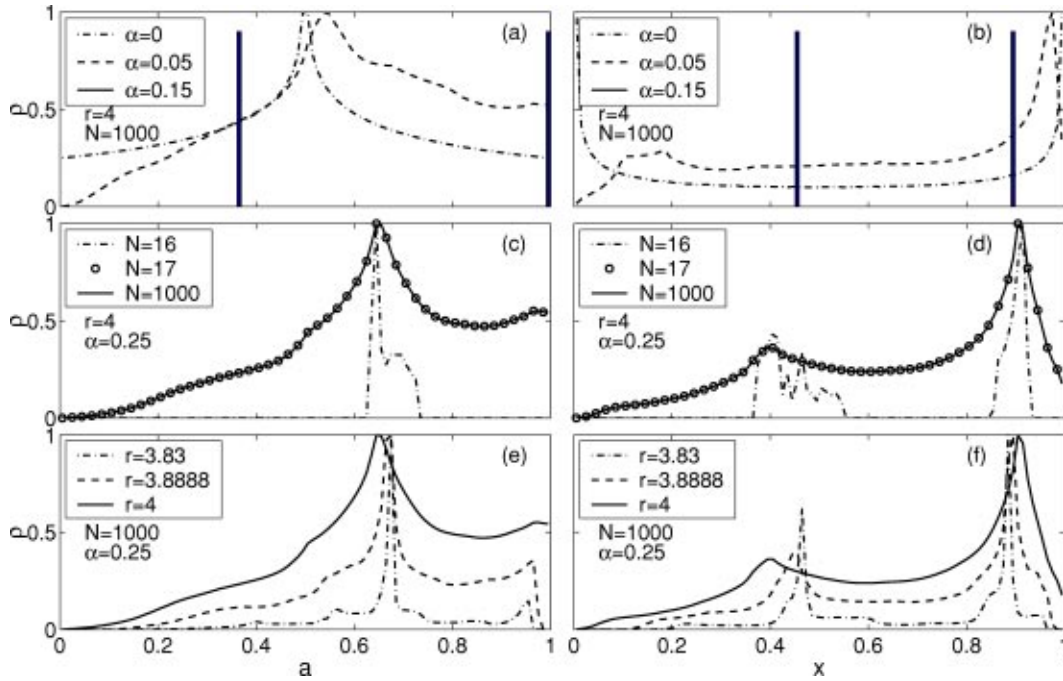
FIG. 7. Densities $\rho(a)$ and $\rho(x)$ of $a(t) = [f(x_{n-1}(t)) + f(x_{n+1}(t))]/2$ [panels (a),(c),(e)] and $x(t)$ [panels (b), (d), (f)] from Eq. (5) normalized by the maximal value. Note that each row of panels corresponds to the same sets of parameters.

± 0.05)–(0.95 ± 0.05). This wider range for the experiment is probably caused by the presence of site disorder.

This confirms that the best functional form for the simulation data is given by the Kohlrausch function.

C. Single-site dynamics

The iterative rule (2) can be viewed as an equation describing the dynamics of a single element in the presence of an external additive perturbation $a(t)$:

$$x(t+1) = (1-\alpha)f(x(t)) + \alpha a(t), \qquad (5)$$

where $a(t) = [f(x_{n-1}(t)) + f(x_{n+1}(t))]/2$. For simplicity, since all sites are statistically identical, we drop the subscript n in Eq. (5).

This form allows us to concentrate on the impact, at the single-site level, of the rest of the network and to try to identify the essential elements for a stretched-exponential dynamics. For this purpose, it is convenient to use the natural invariant density $\rho(x)$ generated by typical orbits $\{x(t)\}$, $t = 1, 2, \ldots$, of the map in Eq. (5). The notion of the natural invariant density is widely used in the studies of chaos [24]. The function $\rho(x)$ is defined so that for any interval $[x, x + dx] \in [0,1]$, the fraction of the time, typical orbits spend in this interval is $\rho(x)dx$. In the same way, one can define the density $\rho(a)$ for the perturbation $a(t)$ in Eq. (5).

Figure 7 shows the behavior of $\rho(a)$ and $\rho(x)$ for a few sets of the parameters α, N, and r. In the case of an isolated map ($\alpha = 0$) and in the chaotic regime, $a(t)$ is the sum of two identically distributed independent random variables— $\rho(a)$ is shown by the dash-dotted line in Fig. 7(b). According to the central limit theorem, if this sum contained much more than two terms, $\rho(a)$ would very well agree with the normal

(Gaussian) distribution. However, even with only two terms, $\rho(a)$ exhibits a maximum at $a = 1/2$ [the dash-dotted line in Fig. 7(a)].

The presence of one or few peaks in $\rho(a)$ makes the orbits $\{x(t)\}$ intermittent for some values of the nonlinearity parameter r. This intermittency means that the (coarse-grained) orbit $\{\sigma(t)\}$, see Eq. (4), stays periodic for some time, becomes chaotic for a certain while, and goes periodic again. In order to demonstrate, how a periodic attractor develops in a coupled system at a value of r, for which the isolated map produces a chaotic orbit, we can imagine a density $\rho(a) = \delta(a - a_0)$, where $\delta(a)$ is the delta function and $a_0 \in [0,1]$ is a constant. In this case, Eq. (5) becomes $x(t+1) = (1-\alpha)f(x(t)) + \alpha a_0 = c_1 f(x(t)) + c_2$, which is the iterative equation for the isolated map scaled by a constant c_1 and shifted by another constant c_2. This manipulation with the isolated map results in a bifurcation diagram translated with respect to the original one [Fig. 3(a)], while preserving all its qualitative features, see Fig. 5. In particular, the period-2 attractors of the modified map overlap with chaotic orbits of the original map.

As discussed above, in the interval $0.1 < \alpha < 0.19$, the lattice falls into period-2 spatial and temporal patterns, i.e., each of the two neighboring sites oscillate out of phase and each site alternates between two values $x^{(1)} < x^{(2)}$, as indicated in Figs. 7(a) and 7(b).

For larger values of α, the natural invariant density becomes more complex. When the lattice size is a small even number, the spatial pattern is periodic with the period, which is equal to four (two sites "up" followed by two sites "down") and each site again undergoes a period-2 dynamics [Figs. 7(c) and 7(d)], which is manifested by the peaks in $\rho(x)$. For $N = 16$, there are narrow peaks in $\rho(a)$ and $\rho(x)$.

These peaks broaden and merge rapidly, however, for large N, and the system displays strong sign of chaoticity.

This chaoticity can be controlled by r, and we see that the orbits spend more and more time in the period-2 attractors relative to the chaotic ones as the nonlinearity parameter is decreased, relating directly to a change in the value of the stretching exponent β [Figs. 7(e) and 7(f)].

Although providing a clearer picture of the dynamics, knowledge of the invariant density is not sufficient to reproduce the stretched-exponential dynamics. For example, choosing randomly the values of $a(t)$ in Eq. (5) according to a prescribed $\rho(a)$ generates only an exponential trap-time distribution. Variations on this theme, including the introduction of a two-step distribution, which favors staying in the period-2 phase once in it, also fail to give a stretched-exponential distribution of trap times. Spatial correlations, even though short range, are essential to induce a stable and self-organized stretched-exponential distribution.

D. Stability of the spatial period-4 structure

Figure 1 plots the time sequence for $\sigma_n(t)$ on a small region of a 1000-site chain for $r=3.83$ ($\beta \approx 0.33$) and $r=3.8888$ ($\beta \approx 0.5$). These show a remarkable range in the trap size: the larger traps of the first one can be up to 250 times longer than those at $r=3.8888$, and corresponding to a time scale 30 000 times larger than the basic time step. This time scale is similar to that observed experimentally [7]. In spite of these very stable traps, for long enough time, all sites display an identical dynamics and no region of the lattice remains frozen.

Looking at the same figure, we also see that, *for a given r*, the trap width appears to be uncorrelated with its length: long traps remain narrow and are composed of ordered domains with several occurrences of period 4, 5, or 6. While the period-4 domains can remain totally stable for a long time, the middle site of the three-up or three-down segment in period-5 and period-6 domains show some instability. They must, therefore, be considered more as defects in the stable phase than as additional spatial structures. Even so, these larger basic domains, that occur mostly for the lower values of r, are responsible for the apparent spatial periodicity of 5 in the spatial correlation function at $r=3.83$ (see Fig. 2).

In view of this discussion, the space-time diagram can be separated in two distinct phases: the ordered spatial period-4 and the chaotic phase. The former can only be destroyed at the boundary or by spatial defects (domains of period 5 or 6).

We verify this observation by two simulations. First, the entire chain is initially set into period-4 state, with the period formed by two neighboring sites with $x_n(0)=x^{(1)}$, $n=1,2$ and the next two sites with $x_n(0)=x^{(2)}$, $n=3,4$. The values $x^{(1)}$ and $x^{(2)}$ are taken to be equal to those corresponding to the two peaks in $\rho(x)$ in Fig. 7(f) for $r=3.83$ and $N=1000$. Simulations starting from these initial conditions remain frozen in these spatial period-4 and temporal period-2 states indefinitely. Although metastable, these states require the presence of defects to be destroyed.
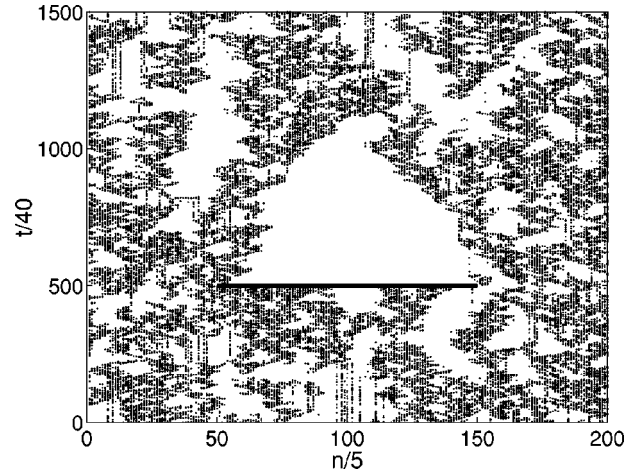

FIG. 8. Space-time diagram for $N=1000$ and $r=3.83$. Dots correspond to trap boundaries—points in time when a site interrupts its temporal period-2 dynamics. Every fifth site and every 40th iteration are shown. The heavy horizontal line shows the region, which was set into the spatial period-4 state at a certain moment in time. Note that the thus induced spatial period-4 domain does not have any bursts in the interior, and is affected by the chaotic phase only at the boundaries.

This can be checked in a second test. We first iterate a 1000-site lattice at $r=3.83$, for 10^6 time steps, in order to eliminate any transient effects. At that point, at once, half of the chain sites are set into the same spatial period-4 state as above. As shown in Fig. 8, this phase then disappears gradually, over about 30 000 time steps, invaded from the edges by the chaotic phase.

V. DISCUSSION

The previous sections have shown that the dynamics of the network can be understood in terms of a competition between two dynamical regimes: a stable period-2 orbit and a fully chaotic state. This can be deduced from Figs. 5 and 7 when the neighboring sites are in opposite bands, their contribution shifts the bifurcation diagram into a period-2 regime. A spatial period 4 is therefore, the basic stable motif with this set of parameters.

As mentioned above, we cannot reconstruct a stretched-exponential dynamics by simply using the natural invariant density inserted into Eq. (5). We have found that the only way to obtain a stretched-exponential trap-time distribution in this situation is to impose a stretched-exponential trap-time distribution on $a(t)$ for the values of a within the peak region in $\rho(a)$ (see Fig. 7). More interestingly, connecting a single site, with a unidirectional coupling, to two sites selected at random on a lattice, is sufficient to induce a stretched-exponential trap distribution on this single site, albeit with a larger β than that for the elements that belong to the lattice.

Thus, once an external perturbation, following a stretched-exponential dynamics, is imposed on a chaotic element, the latter will immediately adopt a similar dynamics. However, stretched-exponential distributions cannot be observed in a self-organized process without spatial organiza-

tion. For example, connecting the nodes of a balanced binary tree unidirectionally towards its root results in the densities $\rho(x)$ and $\rho(a)$, similar to those depicted in Figs. 7(e) and 7(f), already for two levels in the tree. Nevertheless, the trap-time distribution measured at the root node is a pure exponential. This suggests that the stretched-exponential distributions require some spatial organization allowing time-limited, spatial period-4 structures to occur and to be stabilized.

The nature of this spatial organization is somewhat paradoxical. Correlations are very short range and the width of these domains are only weakly varying with the stretching parameter. While traps at $r = 3.83$ are up to 250 times longer than those at $r = 3.8888$, their width is only four to five times larger, as displayed in Fig. 1. This decoupling between spatial and temporal correlation is reminiscent of dynamical heterogeneities observed in glass-forming systems [17,28,29]. Associating a "temperature" with the control parameter r, we see that the spatial size of the traps increases with decreasing r without diverging. In the same way, the size of dynamical heterogeneities increases and the stretching exponent β decreases under cooling in glass-forming systems.

As we also showed that once in a perfect spatial period-4 regime, the system will never become chaotic. The finite lifetime arises from defects in the period-4 phase or from the chaotic boundaries. This behavior is similar to what is seen in the spin-system models with effective constraints on the dynamics [17] and the state-space partition model [30]. Interestingly, both models show a stretched-exponential decay of certain statistical quantities. The distinctive feature of the present model, Sec. II is that the effective dynamical constraints arise in the course of the evolution described by the dynamical equation (2), unlike the above cited models, where the fixed constrains are imposed on the neighboring sites and the dynamics is due to a Monte Carlo procedure.

VI. CONCLUSION

The coupled array of chaotic oscillators presented here has a number of properties that make it an important model. As was shown above and in Ref. [7], it is a faithful representation of the dynamics of an experimental setup of coupled diode resonators in a chaotic regime characterized by a stretched-exponential distribution of trap time. Moreover, the low cost associated with numerically solving the model of Eq. (2) allows us to study the system on time scale unreachable with atomic models; it takes less than a day, on a fast processor, to iterate a lattice of 1000 sites over 10^9 steps. With traps extending to more than 30 000 times the basic time step, long simulations are absolutely necessary to establish the nature of the dynamics in these systems.

Results of these simulations demonstrate that the stretched-exponential distributions arise from the competition between a chaotic and a period-2 regimes. The stretched exponential requires some spatial organization to appear, but does not imply a diverging length scale as the traps become longer and longer: the period-4 structure is sufficient to stabilize a site onto a periodic orbit and the space of the spatial correlation is only weakly related to the length of the traps appearing in these systems.

There are strong similarities between this system and the configurational glasses, and we suggest that the understanding gained here could be extended directly to these important materials. We are currently pursuing this avenue of research.

[1] J. C. Phillips, Rep. Prog. Phys. **59**, 1133 (1996).

[2] I. Campbell, J. Plasma Phys. **46**, L1159 (1985).

[3] M. Dzugutov and J. Phillips, J. Non-Cryst. Solids **192-193**, 397 (1995).

[4] M. Donsker and S. Varadhan, Commun. Pure Appl. Math. **28**, 525 (1975); **32**, 721 (1979); **28**, 677(E) (1975).

[5] P. Grassberger and I. Procaccia, J. Chem. Phys. **77**, 6281 (1982).

[6] G. Barkema, P. Biswas, and H. van Beijeren, Phys. Rev. Lett. **87**, 170601 (2001).

[7] E. Hunt, P. Gade, and N. Mousseau, e-print cond-mat/0204179.

[8] M. Roy and R. E. Amritkar, Phys. Rev. E **55**, 2422 (1997).

[9] P. Pruthi, Ph.D. thesis, Royal Institute of Technology, Stockholm, Sweden, 1995 (unpublished), URL: http://www.niksun.com/publications/parag_thesis/index.htm.

[10] U. Frisch and D. Sornette, J. Phys. I **7**, 1155 (1997).

[11] A. Gamba and I. Kolokolov, J. Stat. Phys. **94**, 759 (1997).

[12] W. Weibull, J. Appl. Mech. **18**, 293 (1951).

[13] J. Laherrére and D. Sornette, Eur. Phys. J. B **2**, 525 (1998).

[14] A. K. Jonscher, J. Phys. D **32**, R57 (1999).

[15] By analogy, the case $1 < \beta < 2$ is often called "stretched Gaussian" (see, e.g., Refs. [31,32]).

[16] G. Gielis and C. Maes, Europhys. Lett. **31**, 1 (1995).

[17] J. P. Garrahan and D. Chandler, Phys. Rev. Lett. **89**, 035704 (2002).

[18] G. A. Johnson, M. Löcher, and E. R. Hunt, Physica D **96**, 367 (1996).

[19] M. Löcher, D. Cigna, E. R. Hunt, G. A. Johnson, F. Marchesoni, L. Gammaitoni, M. E. Inchiosa, and A. R. Bulsara, Chaos **8**, 604 (1998).

[20] M. Löcher, D. Cigna, and E. R. Hunt, Phys. Rev. Lett. **80**, 5212 (1998).

[21] M. Löcher, N. Chatterjee, F. Marchesoni, W. L. Ditto, and E. R. Hunt, Phys. Rev. E **61**, 4954 (2000).

[22] R. W. Rollins and E. R. Hunt, Phys. Rev. A **29**, 3327 (1984).

[23] C. E. Elmer and E. S. V. Vleck, SIAM (Soc. Ind. Appl. Math.) J. Appl. Math. **61**, 1648 (2001).

[24] E. Ott, *Chaos in Dynamical Systems* (Cambridge University Press, Cambridge, 1993).

[25] C. Godréche and J. M. Luck, J. Stat. Phys. **104**, 489 (2001).

[26] J.-P. Hansen and I. R. McDonald, *Theory of Simple Liquids*, 2nd ed. (Academic Press, London, 1986).

[27] S. Simdyankin, N. Mousseau, and C. Godrèche (unpublished).

[28] K. Vollmay-Lee, W. Kob, K. Binder, and A. Zippelius, J. Chem. Phys. **116**, 5158 (2002).

[29] M. Dzugutov, S. I. Simdyankin, and F. H. M. Zetterling, Phys. Rev. Lett. **89**, 195701 (2002).

[30] W. Nadler, T. Huang, and D. L. Stein, Phys. Rev. E **54**, 4037 (1996).

[31] L. Kaplan and E. Heller, Phys. Rev. Lett. **76**, 1453 (1996).

[32] J. van Zon and F. MacKintosh, e-print cond-mat/0205512.